

Structural and magnetoresistive properties of magnetic tunnel junctions with half-metallic Co₂MnAl

J. J. Qiu,^{1,a)} G. C. Han,¹ W. K. Yeo,¹ P. Luo,¹ Z. B. Guo,¹ and T. Osipowicz²

¹Data Storage Institute, DSI Building, 5 Engineering Drive, Singapore 117608, Singapore

²Department of Physics, National University of Singapore, Lower Kent Ridge Road, Singapore 119260, Singapore

(Presented on 8 November 2007; received 11 September 2007; accepted 11 October 2007; published online 22 January 2008)

A series of polycrystalline full-Heusler Co₂MnAl thin films were deposited on Si (100) coated with thermo SiO₂ by using different types of seed layers such as Cr, Mg, MgO/Cr, and MgO. The properties of the Co₂MnAl thin films such as the coercivity, atomic composition, and crystalline structure strongly depend on the deposition conditions and seed layers. Very soft Co₂MnAl thin films with coercivity of 8.3 Oe and small magnetostriction coefficient $\lambda_S=1.43 \times 10^{-5}$ had been obtained when MgO was used as seed layer. Magnetic tunnel junctions with magnetoresistance ratio of 12%–19% by utilizing the Co₂MnAl as bottom ferromagnetic electrode have been successfully fabricated. © 2008 American Institute of Physics. [DOI: 10.1063/1.2830554]

I. INTRODUCTION

Half-metallic ferromagnets (HMFs) which have only one spin-band electron at Fermi energy have promising potential for application to spintronics device such as magnetic tunnel junctions (MTJs) as electrodes. According to Julliere's model, MTJs using HMFs as electrodes would have extraordinarily large magnetoresistance ratios (MRs).¹ Co-based full-Heusler alloy X_2YZ compounds (Co₂MnSi, Co₂MnGe, Co₂CrFeAl, etc.) have attracted much interest because of their predicted half-metallic band structure and high Curie temperatures.^{2–4}

Full-Heusler alloys belong to a group of ternary intermetallic compounds of general formula X_2YZ with a $L2_1$ structure. Full-Heusler alloys also have $B2$ and $A2$ structures depending on their site-disordered state, in which (Y,Z) and (X,Y,Z) are randomly substituted, respectively. According to theoretical calculations, the spin polarization of $L2_1$ -ordered full-Heusler alloy is very sensitive to site disordering because the upper and lower edge states of the minority band gap are derived from localized antibonding states on the Co site. It is difficult to fabricate $L2_1$ -ordered full-Heusler alloy films with no structural imperfections.^{5,6} Heating to high temperatures (400–600 °C) is necessary for full-Heusler alloys to form a highly ordered $L2_1$ structure, but the temperatures over 400 °C for top electrodes are generally undesirable because of the problem of heat endurance in MTJs. Co₂MnAl is an attractive compound because large spin polarization of 0.76 is expected even in a $B2$ structure that can be obtained easily through heating at lower temperatures (200–300 °C).⁷

In this paper, we will report characterization of a series of full-Heusler alloy Co₂MnAl (CMA) thin films deposited on Si (100) coated with thermo-SiO₂ substrate under different deposition conditions. Firstly, we studied the influence of

seed layer on magnetic properties and crystalline structure of CMA films by using different types of seed layers such as Cr, Mg, MgO/Cr, and MgO. Then, the effects of deposition conditions such as Ar sputtering pressure, rf power, and substrate temperature were also studied. Very soft CMA thin films with coercivity of 8.3 Oe and small magnetostriction coefficient $\lambda_S=1.43 \times 10^{-5}$ have been obtained under optimized deposition conditions when MgO is used as seed layer. MTJs with MR ratio of about 19% by utilizing the CMA as the bottom ferromagnetic electrode have been successfully fabricated.

II. EXPERIMENTAL PROCEDURE

All films were grown on Si(100) coated with a 1 μm thickness of a thermally oxidized SiO₂ substrate by using an ultrahigh vacuum sputtering system with a base pressure of about 5×10^{-10} Torr. Some detailed information about the deposition system can be found in Ref. 8. All layers were deposited at room temperature under 0.1 Pa Ar pressure except the CMA layer which was deposited at different temperature and Ar pressure by using a sintered alloy Co₄₄Mn₃₂Al₂₄ target. About 100 Oe electrical magnetic field was applied to the plane of the wafer during deposition for all layers except the MgO layer. The films can be annealed *in situ* or *ex situ* at different temperatures.

Magnetic tunnel junctions were fabricated according to the following steps: (1) Deposition of a film stack with the structure of MgO(30)/CMA(50)/Mg(0.3) (thickness unit in nanometer) on 4 in. Si wafer coated with 1- μm -thick SiO₂. (2) About 0.7–0.9 nm MgO junction layer was deposited by using a sintered MgO target under plasma oxidation and after that a top synthetic-type-ferromagnetic electrode with the structure of CoFe(3.5)/Ru(0.8)/CoFe(4)/IrMn(12)/Ta(10) was deposited above the MgO layer. (4) Photolithography patterning and ion-milling technique were used to fabricate the magnetic tunneling junctions. Contact via hole was opened by using self-alignment method. (5) After completion

^{a)}Author to whom correspondence should be addressed. Electronic mail: qiu_jinjun@dsi.a-star.edu.sg.

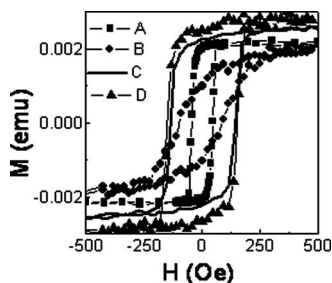


FIG. 1. M - H curves of seed layer/Co₂MnAl(30)/Cr(3) with different seed layers: (A) MgO (20 nm) (square), (B) Mg (25 nm) (circle), (C) Cr (40 nm) (solid line), and (D) MgO(10)/Cr(40) (up triangle).

of the MTJ fabrication, magnetic annealing was carried out in a high vacuum magnetic annealing oven with magnetic field of 1 T and at different annealing temperatures for 2 h to get crystalline MgO junction layer.

Rutherford back scattering (RBS) and x-ray photoelectron spectroscopy (XPS) was used to test the CMA films' composition. Vibrating sample magnetometer (VSM) was used to characterize the magnetic properties. X-ray diffraction (XRD) was used to characterize the crystalline structure. The surface roughness was investigated using atomic force microscope (AFM). MR ratio of the MTJs was measured by using four-probe method with the variable magnetic field. Magnetostriction was measured using an automated cantilever-beam Lafouda tester at a rotating field of 50 Oe applied along the film surfaces.

III. RESULTS AND DISCUSSION

Seed layer is a key factor to influence the characteristic of CMA films. Cr, Mg, Ta, MgO, Ru, Ta/NiFe, etc., were tested as seed layers for CMA films. Figure 1 just shows M - H curves of 30 nm CMA films with four different seed layers: (A) MgO (20 nm) (square), (B) Mg (25 nm) (circle), (C) Cr (40 nm) (solid line), and (D) MgO(10)/Cr(40) (up triangle). All samples were deposited at room temperature under Ar gas sputtering pressure of 0.3 Pa and rf power of 100 W, then postannealed at 400 °C for 2 h with 1 T field applied. Differences in magnetization moment for these four samples were caused by the variation of the sample size. Their coercivities were 45.67, 90.29, 142, and 147 Oe, respectively. Moreover, their squarenesses are 0.928, 0.423, 0.845, and 0.854, respectively. Among these four samples, type A with 20 nm MgO as seed layer had the best magnetic properties with the smallest coercivity and biggest squareness for application in MTJs, so the MgO was chosen as the seed layer.

XRD results explained why MgO is the best seed layer for CMA films. Figure 2 shows two XRD patterns for CMA thin films deposited on MgO and Cr seed layers under the same conditions. Both as-deposited films on MgO and Cr seed layers were amorphous. After annealing at 400 °C for 2 h, the Cr seed layer and the above CMA thin film changed into polycrystalline structure and Cr (110), Cr (200), and CMA (400) peaks were tested [Fig. 2(a)], whereas only the MgO (200), the CMA (200), and CMA (400) peaks were

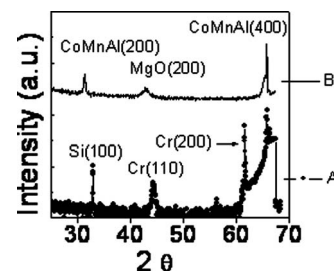


FIG. 2. XRD patterns of CoMnAl films: (A) Cr(40)/CMA(30)/Cr(3) (circle) and (B) MgO(40)/CoMA(60)/Cr(3) (solid line).

observed in the CMA sample with MgO as seed layer [Fig. 2(b)] indicating perfect CMA (100) oriented growth on MgO seed layer

Figure 3 shows M - H curves of 400 °C annealed MgO(20)/CoMA(30)/Cr(3) films which were deposited at room temperature under rf power of 100 W with three types of Ar gas sputtering pressure: 0.1 Pa (square), 0.3 Pa (solid line), and 0.47 Pa (up triangle). As the sputtering pressure changes from 0.1 to 0.3 Pa, the squareness increased from 0.836 to 0.928 and coercivity decreased from 64.34 to 45.67 Oe, which indicated that magnetic properties of CMA film deposited at 0.3 Pa were better than at 0.1 Pa. The atomic compositions of CoMnAl films deposited at 0.1 and 0.3 Pa tested by RBS were Co(0.47)Mn(0.305)Al(0.219) and Co(0.475)Mn(0.285)Al(0.240), respectively. The latter ratio was closer to 2:1:1. While the sputtering pressure changed to 0.47 Pa, the coercivity decreases to 17.07 Oe, whereas the squareness decreased to 0.735. The magnetic properties deteriorated comparing with that of 0.3 Pa. RBS indicated that the atomic composition of CMA changed into Co(0.453)Mn(0.306)Al(0.241) which was worse than that of the CMA deposited at 0.3 Pa. 0.3 Pa was chosen to deposit the CMA films.

Figure 4 shows M - H curves of 400 °C annealed MgO(20)/CoMA(30)/Cr(3) films deposited at room temperature under sputtering Ar gas pressure of 0.3 Pa with different rf powers applied. As the power increased from 50 to 200 W, the coercivity decreased monotonously from 83.2 to 18.6 Oe, whereas the squareness increased monotonously from 0.83 to 0.97. Higher power improved the properties of CMA films. 200 W was chosen for deposition of CMA layer since 200W is the maximum rf power supply of the sputter system.

Substrate temperature is also an important factor to influence the characteristic of CMA films. Room temperature

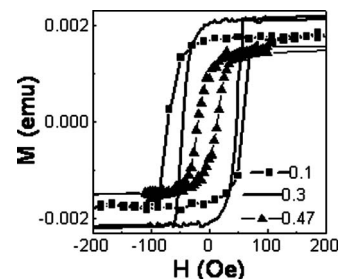


FIG. 3. M - H curves of MgO(20)/CoMA(30)/Cr(3) films deposited at different sputtering pressures: 0.1 Pa (square), 0.3 Pa (solid line), and 0.47 Pa (up triangle).

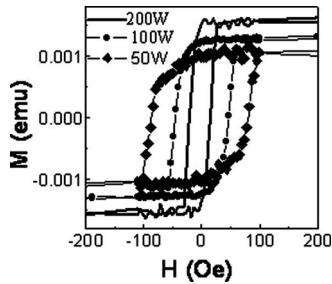


FIG. 4. M - H curves of MgO(20)/CoMA(30)/Cr(3) films deposited with different rf powers: 50 W (diamond), 100 W (circle), and 200 W (solid line).

and 200 °C were tested to deposit the CMA films. Very soft CoMnAl thin films with coercivity of 8.3 Oe (shown in insert of Fig. 5) and small magnetostriction coefficient $\lambda_S = 1.437 \times 10^{-5}$ had been obtained (showed in Fig. 5) when the CMA film was deposited at 200 °C under sputtering pressure of 0.3 Pa and rf power of 200 W, and MgO is used as seed layer. λ_S was just about two times as that of Co₉₀Fe₁₀ films.⁹

Figure 6 shows the M - H curves of as-deposited (solid square) and 300 °C annealed for 2 h (solid line) MTJs with structure of MgO(30)/CoMA(50)/MgO(1.0)/CoFe(3.5)/Ru(0.8)/CoFe(4)/IrMn(12)/Ta(10) and relative minor MR loops (inserted figures). The junction area was about $60 \times 60 \mu\text{m}^2$. The MR ratio and RA of as-deposited MTJ were 7% and $700 \Omega \mu\text{m}^2$, respectively. After annealing at 300 °C for 2 h in vacuum with 1 T magnetic field applied, the RA increased slightly to $750 \Omega \mu\text{m}^2$, whereas the MR ratio increased significantly to 19%. The coercivity of free layer CMA decreased from 180 to 100 Oe. The interlayer coupling (H_{in}) between free layer CMA and pinned layer increased from 10 to 25 Oe. The small change in RA and H_{in} enhancement indicated a decrease in the junction thickness after 300 °C annealing. 350 °C was also used to anneal the sample, MR ratio decreased to 12% and RA increased to $1040 \Omega \mu\text{m}^2$. The H_{in} decreased to 5 Oe. According to the results of CMA films, the best annealing temperature for CMA film was 400 °C. Since the MTJs were top-type pinned by IrMn which could not endure high annealing temperature, *in situ* annealing at 400 °C after CMA or MgO junction deposition will be tested in future. The 19% MR ratio is much smaller than that of either our prepared AlO MTJs with conventional Co₉₀Fe₁₀ electrodes,¹⁰ or MTJs of Sakuraba *et al.* with epitaxial CoMnAl electrode⁷ are mainly due to the rough surface of bottom electrode MgO(30)/

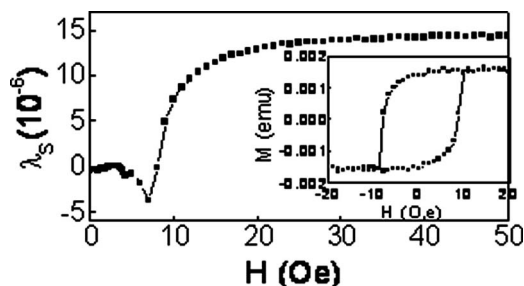


FIG. 5. Magnetostriction of MgO(20)/CoMA(30)/Cr(3) deposited at 200 °C (the inserted figure is relative M - H curve).

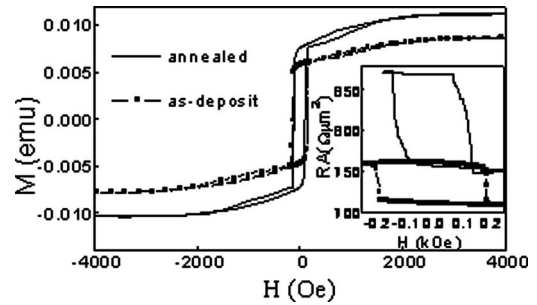


FIG. 6. M - H curves of as-deposited (solid square) and 300 °C annealed (solid line) MTJ with structure of MgO(30)/CoMA(50)/MgO(1.0)/CoFe(3.5)/Ru(0.8)/CoFe(4)/IrMn(12)/Ta(10) and relative minor MR loops (inserted).

CoMnAl(50). AFM shows that the roughnesses (R_{MS}) of bottom electrode and MTJ are 2.017 and 1.854 nm, respectively. The R_{MS} of bottom electrode is far higher than that of 0.283 nm (Ref. 10) and 0.2 nm.⁷ The atomic composition of CoMnAl deviation from the standard Heusler alloy ratio of 2:1:1 will also reduce the MR ratio of MTJ.

IV. CONCLUSION

In summary, full-Heusler alloy Co₂MnAl thin films deposited on Si (100) coated with thermo-SiO₂ substrate under different deposition conditions such as seed layer, Ar sputtering pressure, rf power, and substrate temperature were studied. Very soft (100) oriented Co₂MnAl thin films with coercivity of 8.3 Oe and small magnetostriction coefficient $\lambda_S = 1.437 \times 10^{-5}$ had been obtained under optimized deposition conditions when MgO was used as seed layer. IrMn pinned top-type MTJs by utilizing the CoMnAl as the bottom ferromagnetic electrode have been successfully fabricated and the MR ratio was 19%.

ACKNOWLEDGMENTS

The authors would like to thank Mr. Joon Fatt Chong and Dr. Hu Jiangfeng for their help in XRD measurement. The authors also appreciate Ms. Archana Balakrishnan's assistant in CMS thin film heat treatment and VSM characterization. Partial support from Information Storage Industry Consortium is acknowledged.

¹M. Julliere, Phys. Lett. **54A**, 225 (1975).

²T. Ambrose, J. J. Krebs, and G. A. Prinz, J. Appl. Phys. **89**, 7522 (2001).

³T. Ishikawa, T. Marukame, S. Hakamata, K.-I. Matsuda, T. Uemura, and M. Yamamoto, J. Magn. Magn. Mater. **310**, 1897 (2007).

⁴H. Kijima, T. Ishikawa, T. Marukame, K.-I. Matsuda, T. Uemura, and M. Yamamoto, J. Magn. Magn. Mater. **310**, 2006 (2007).

⁵S. B. Ravel, M. P. Raphael, Q. Huang, and V. G. Harris, Phys. Rev. B **65**, 184431 (2002).

⁶S. B. Ravel, J. O. Cross, M. P. Raphael, V. G. Harris, R. Ramesh, and V. Saraf, Appl. Phys. Lett. **81**, 2812 (2002).

⁷Y. Sakuraba, J. Nakata, M. Oogane, Y. Ando, H. Kato, A. Sakuma, T. Miyazaki, and H. Kubota, Appl. Phys. Lett. **88**, 022503 (2006).

⁸K. B. Li, Y. H. Wu, J. J. Qiu, G. C. Han, Z. B. Guo, H. Xie, and T. C. Chong, Appl. Phys. Lett. **79**, 3663 (2001).

⁹J. J. Qiu, G. C. Han, K. B. Li, Z. Y. Liu, B. Y. Zong, and Y. H. Wu, J. Appl. Phys. **99**, 094304 (2006).

¹⁰K. B. Li, Y. H. Wu, J. J. Qiu, G. C. Han, Z. B. Guo, and T. C. Chong, J. Magn. Magn. Mater. **241**, 89 (2002).